Supplementary Information: Entanglement Activation in Multiphoton Distillation Networks

Here, we provide supplementary information for the theory of entanglement activation and experimental setup. In Sec. I, we give background knowledge to multipartite entanglement. In Sec. II, we provide methods to verify the genuine multipartite entanglement (GME) and stochastic localizable entanglement (SLE) of a given state. In Sec. III, we use these methods to verify the GME and SLE of to-be-distilled states in our experiment. In Sec. IV, we take the ideal Werner state as an example to prove the existence of SLE activation phenomenon theoretically. In Sec. V, we provide an experimental analysis of how the distillation scheme works. In Sec. VI, we further explain the Werner state preparation process. In Sec. VII, we list all the reconstructed density matrices from quantum tomography.

CONTENTS

I. BACKGROUND

We first give some basic definitions which will be frequently used in this work. An N-partite state ρ is said to be bi-separable if it can be written as

$$\rho = \sum_{g\subset[N]} \sum_{i} p_{gi} \rho_g^i \otimes \rho_{\bar{g}}^i, \tag{S1}$$

where g denotes a nontrivial subset of the N parties, $\bar{g} = [N] - g$ is the complementary of g, $\{p_{gi}\}_{g,i}$ is a probability distribution satisfying $\sum_{g,i} p_{g,i} = 1$ and $p_{gi} \geq 0$, ρ_g^i and $\rho_{\bar{g}}^i$ are quantum states defined on systems g and $\bar{g}$. If an N-partite state ρ cannot be decomposed into this form, it is a genuinely multipartite entangled state. It is worth mentioning that a bi-separable state may also have quantum resources. For example, it can be entangled with respect to a given bi-partition.

Local operations and classical communication (LOCC) can be written in a separable form [1]

$$\Lambda(\rho) = \sum_i \left(K_1^i \otimes \cdots \otimes K_N^i\right) \rho \left(K_1^i \otimes \cdots \otimes K_N^i\right)^\dagger, \tag{S2}$$

where ρ is an N-partite quantum state and K denotes the Kraus operator satisfying

$$\sum_i \left(K_1^i \otimes \cdots \otimes K_N^i\right)^\dagger \left(K_1^i \otimes \cdots \otimes K_N^i\right) = \mathbb{I}. \tag{S3}$$

Stochastic local operations and classical communication (SLOCC) are defined based on LOCC, which permits post-selection of the resultant states in Eq. (S2). Thus, SLOCC can also be written as the separable form of Eq. (S2) with

$$\sum_i \left(K_1^i \otimes \cdots \otimes K_N^i\right)^\dagger \left(K_1^i \otimes \cdots \otimes K_N^i\right) \leq \mathbb{I}. \tag{S4}$$

Due to the stochastic property, a SLOCC operation may succeed with a probability less than 1.

It can be proved that neither LOCC nor SLOCC can distillate GME from one copy of a bi-separable state. As for bi-separable state ρ,

$$\Lambda(\rho) = \sum_{g\in[N]} \sum_i p_{gi} \sum_j \left(K_1^j \otimes \cdots \otimes K_N^j\right) \rho_g^i \otimes \rho_{\bar{g}}^i \left(K_1^j \otimes \cdots \otimes K_N^j\right)^\dagger \tag{S5}$$

is also a bi-separable state with a form similar to Eq. (S1).

It is shown that the simultaneous preparation of multiple bi-separable states can activate GME [2]. For example, if we collect two bi-separable tripartite states σ_{ABC} and $\sigma'_{A'B'C'}$ and regard them as a whole to be a new tripartite state $\rho_{AA',BB',CC'} = \sigma_{ABC} \otimes \sigma'_{A'B'C'}$, this new state can have tripartite GME over the partition AA', BB', and CC'.

II. GME AND SLE VERIFICATION

As the theme of our work is entanglement activation, including GME and SLE activation, it is necessary to ensure that to-be-distilled states have no GME and SLE. In the main context, we adopt two fidelity-based entanglement witnesses to show the absence of these two properties, which are not perfect. To further ensure the absence, we need more rigorous GME and SLE verification methods, which will be discussed in this section.

For a general multipartite state, verifying the existence of GME is challenging, and verifying the absence of GME is even more challenging. In theory, necessary and sufficient conditions of GME exist for some density matrices with special forms. For example, every "X"-shape density matrix is entangled if and only if its GME concurrence is larger than 0 [3, 4]. Here, a density matrix is said to be of "X"-shape if we can write it as a form of

$$\rho = \begin{bmatrix} M_1 & M_2 \\ M_2^\dagger & M_3 \end{bmatrix}, \tag{S6}$$

where M_1, M_2, and M_3 are square matrices satisfying $M_1 = \mathrm{diag}(a_1, \cdots, a_L)$, $M_3 = \mathrm{diag}(b_L, \cdots, b_1)$, and $M_2 = \mathrm{antidiag}(c_1, \cdots, c_L)$. The GME concurrence for this state is

$$C_{\mathrm{GME}}\left(\begin{bmatrix} M_1 & M_2 \\ M_2^\dagger & M_3 \end{bmatrix}\right) = 2 \max_i \{0, |c_i| - \sum_{j\neq i} \sqrt{a_j b_j}\}. \tag{S7}$$

We introduce the GME concurrence method for "X"-shape density matrices because our target states, including the ideal Werner state, the distilled Werner state, and the Werner state with bit-flip and phase-flip errors, all have "X"-shape density matrices. However, due to unpredictable noises, real density matrices may deviate from the ideal "X"-shape matrices. So here, we also introduce another GME verification method for states with general forms of density matrices. If the solution of the following semidefinite programming problem for a tripartite state ρ_{ABC} is negative, then ρ_{ABC} is genuinely multipartite entangled [5],

$$\begin{aligned}
&\min_{W} \operatorname{tr}(W\rho_{ABC}) \\
&\text{s.t. } \operatorname{tr}(W) = 1, \\
&\quad W = P_1 + Q_1^{\mathrm{T}_A} \ , \ P_1 \geq 0 \ , \ Q_1 \geq 0, \\
&\quad W = P_2 + Q_2^{\mathrm{T}_B} \ , \ P_2 \geq 0 \ , \ Q_2 \geq 0, \\
&\quad W = P_3 + Q_3^{\mathrm{T}_C} \ , \ P_3 \geq 0 \ , \ Q_3 \geq 0,
\end{aligned} \tag{S8}$$

where T_A denotes the partial transposition operation for indices belonging to subsystem A. This criterion is generalized from the PPT criterion [6] for bipartite entanglement verification. It is worth noting that most entanglement criteria, including this, are sufficient but not necessary conditions. If the solution of this optimization problem is positive for some state ρ_{ABC}, we cannot be sure that this state is bi-separable. Nonetheless, as PPT is a powerful entanglement criterion, the positive value of this optimization problem provides strong evidence for bi-separability. In this work, we will use this PPT-based criterion as evidence for GME of a given tripartite state.

We can reduce the certification of SLE to a bipartite entanglement certification problem based on the theorem derived in the Methods section. Specifically, to certify if a tripartite state ρ_{ABC} has SLE on subsystems A and B, we can use the following function

$$\mathcal{E}_{\mathrm{SL}}(\rho_{ABC}) = \max_{\psi_C} \mathcal{E}\left(\frac{\langle\psi_C|\,\rho_{ABC}\,|\psi_C\rangle}{\operatorname{tr}(\langle\psi_C|\,\rho_{ABC}\,|\psi_C\rangle)}\right), \tag{S9}$$

where $\mathcal{E}(\cdot)$ is a bipartite entanglement quantifier. If A and B are two qubits, we can assign $\mathcal{E}(\cdot)$ to be the entanglement negativity $\mathcal{N}(\rho_{AB}) = \log\left(\operatorname{tr}|\rho_{AB}^{\mathrm{T}_B}|\right)$, which is defined by the violation of PPT criterion [6]. In this case, ρ_{ABC} has SLE on A and B if and only if $\mathcal{E}_{\mathrm{SL}}(\rho_{ABC}) > 0$, as PPT criterion is the necessary and sufficient condition for two-qubit entanglement.

III. GME AND SLE ANALYSIS FOR NOISY INITIAL STATES

To show that we realize the GME and SLE activation in our experiments, we need to prove the absence of GME in to-be-distilled noisy states of $p = 0.5$ and the absence of SLE in to-be-distilled noisy states of $p = 0.36$, as shown in Fig. 3 of the main context. Due to the unavoidable noise in the experimental platform, we cannot prepare ideal Werner states. We mainly adopt two methods to describe these noisy states. The first is based on our knowledge of errors in experiments. In preparing the GHZ state, we know that dominant errors are phase-flip and bit-flip, which can convert the ideal GHZ state $\left|G_0^+\right\rangle$ into seven other GHZ states. All these eight GHZ states are listed as following

$$\begin{aligned}
\left|G_0^\pm\right\rangle &= \frac{1}{\sqrt{2}}(|000\rangle + |111\rangle), \\
\left|G_1^\pm\right\rangle &= \frac{1}{\sqrt{2}}(|001\rangle + |110\rangle), \\
\left|G_2^\pm\right\rangle &= \frac{1}{\sqrt{2}}(|010\rangle + |101\rangle), \\
\left|G_3^\pm\right\rangle &= \frac{1}{\sqrt{2}}(|100\rangle + |011\rangle).
\end{aligned} \tag{S10}$$

Because of the symmetry in light paths, we assume three photons have the same error rate. Thus, we can use three parameters to describe the to-be-distilled states that we actually prepare

$$\rho = p\left[r\rho_0 + \frac{1-r}{3}\left(\rho_1 + \rho_2 + \rho_3\right)\right] + (1-p)\frac{\mathbb{I}_3}{8}, \tag{S11}$$

where $\rho_i = q\left|G_i^+\right\rangle\!\left\langle G_i^+\right| + (1-q)\left|G_i^-\right\rangle\!\left\langle G_i^-\right|$, p, and q, and r are parameters representing rates of white noise, phase-flip error, and bit-flip error, respectively.

In addition to the noise model, we performed quantum tomography on to-be-distilled states. Thus, we can use reconstructed density matrices shown in Sec. VII to analyze the GME and SLE. It is worth mentioning that, due to experimental errors in quantum tomography, the reconstructed density matrix may not be closer to the real state than the noise model, Eq. (S11). Therefore, it is meaningful to adopt both methods to analyze the existence of GME and SLE.

We start from the GME analysis of two to-be-distilled states of $p = 0.5$. Firstly, with the noise model in Eq. (S11), the density matrix of ρ is

$$\rho = \begin{bmatrix} \frac{1-p}{8}+\frac{1}{2}pr & 0 & 0 & 0 & 0 & 0 & 0 & pr(q-\frac{1}{2}) \\ 0 & \frac{1}{8}+\frac{p-4pr}{24} & 0 & 0 & 0 & 0 & \frac{1-r}{3}p(q-\frac{1}{2}) & 0 \\ 0 & 0 & \frac{1}{8}+\frac{p-4pr}{24} & 0 & 0 & \frac{1-r}{3}p(q-\frac{1}{2}) & 0 & 0 \\ 0 & 0 & 0 & \frac{1}{8}+\frac{p-4pr}{24} & \frac{1-r}{3}p(q-\frac{1}{2}) & 0 & 0 & 0 \\ 0 & 0 & 0 & \frac{1-r}{3}p(q-\frac{1}{2}) & \frac{1}{8}+\frac{p-4pr}{24} & 0 & 0 & 0 \\ 0 & 0 & \frac{1-r}{3}p(q-\frac{1}{2}) & 0 & 0 & \frac{1}{8}+\frac{p-4pr}{24} & 0 & 0 \\ 0 & \frac{1-r}{3}p(q-\frac{1}{2}) & 0 & 0 & 0 & 0 & \frac{1}{8}+\frac{p-4pr}{24} & 0 \\ pr(q-\frac{1}{2}) & 0 & 0 & 0 & 0 & 0 & 0 & \frac{1-p}{8}+\frac{1}{2}pr \end{bmatrix}, \tag{S12}$$

which is clearly an "X"-shape density matrix. Thus, to decide whether it is genuinely entangled or not, we only need to calculate the GME concurrence,

$$C_{\mathrm{GME}}(\rho) = 2\max\{0, pr(q-\frac{1}{2}) - \frac{3}{8} - \frac{p-4pr}{8}, \frac{1}{3}p(1-r)(q-\frac{1}{2}) - \frac{1-p}{8} - \frac{pr}{2} - \frac{1}{4} - \frac{p-4pr}{12}\}. \tag{S13}$$

Using the reconstructed density matrix of Fig. S3, we find that the parameters of two initial states are approximately $(p, q, r) = (0.5, 0.9084, 0.9210)$ and $(0.5, 0.9124, 0.9129)$. Substituting them into Eq. (S13), GME concurrences are $2\max\{0, -0.0192, -0.4255\} = 0$ and $2\max\{0, -0.0210, -0.4243\} = 0$, which show that these two states have no GME.

We can also directly use the reconstructed density matrices from quantum tomography to analyze the GME. As reconstructed density matrices are not strict "X"-shape matrices, calculating GME concurrence is challenging [3]. We thus use the PPT-based GME verification method in Eq. (S8) to test these two states. We input reconstructed density matrices of the two to-be-distilled states, shown in Fig. S4, into this optimization problem and solve it numerically. Results are 0.0096 and 0.0066 for two density matrices. These two values are all greater than 0, so this PPT-based verification method cannot detect their GME. As this method does not ask for an "X"-shape density matrix and the PPT criterion is a strong entanglement criterion, these results provide strong evidence that to-be-distilled states have no GME.

We now analyze the SLE of to-be-distilled states with $p = 0.36$ based on the theorem developed in the Methods section of the main context. Here, we numerically verify SLE by searching over all single-qubit pure states $|\psi_C\rangle = \cos\theta\,|0\rangle + \sin\theta e^{i\phi}\,|1\rangle$ to find a positive value of $\mathcal{E}_{\mathrm{SL}}(\rho_{ABC})$ defined in Eq. (S9), where $\mathcal{E}(\cdot)$ is chosen to be entanglement negativity. We numerically calculate that the noisy state in Eq. (S11) with parameters $(p, q, r) = (p, 0.9084, 0.9210)$ has no SLE when $p < 0.4095$ and the state with parameters $(p, q, r) = (p, 0.9124, 0.9129)$ has no SLE when $p < 0.4103$. This shows that two to-be-distilled states with $p = 0.36$ have no SLE. We also directly use reconstructed density matrices shown in Fig. S5 to prove the absence of SLE. After calculation, values of $\mathcal{E}_{\mathrm{SL}}(\rho_{ABC})$ of these two to-be-distilled states are both 0. To further consolidate this conclusion, we change $\mathcal{E}(\cdot)$ to be the lowest eigenvalue of the input bipartite density matrix after partial transposition, $\mathcal{E}(\rho_{AB}) = \lambda_{\min}(\rho_{AB}^{\mathrm{T}_B})$. In this case, if $\mathcal{E}_{\mathrm{SL}}(\rho_{ABC})$ is larger than 0, ρ_{ABC} has no SLE. We numerically calculate the values of $\mathcal{E}_{\mathrm{SL}}(\rho_{ABC})$ for two to-be-distilled states to be 0.036 and 0.029, which confirms the absence of SLE in these two states.

IV. GME AND SLE ACTIVATION FOR THE WERNER STATE

The Werner state has a simple mathematical form and entanglement structure. We can use it as a theoretical example to analyze the activation of GME and SLE. The Werner state is parameterized by a single parameter p as

$$\rho_{\mathrm{werner}} = p\left|G_0^+\right\rangle\!\left\langle G_0^+\right| + \frac{1-p}{8}\mathbb{I}_3, \tag{S14}$$

which is apparently an "X"-shape density matrix, with GME concurrence

$$C_{\mathrm{GME}}(\rho_{\mathrm{werner}}) = 2\max\{0, \frac{7}{8}p - \frac{3}{8}\}. \tag{S15}$$

Thus, the Werner state is genuinely multipartite entangled if and only if $p > \frac{3}{7}$. After the distillation procedure shown in Sec. V, the ideal Werner state becomes

$$\rho'_{\text{werner}} = \frac{1}{3p^2+1}\begin{bmatrix} \frac{(3p+1)^2}{8} & 0 & 0 & 0 & 0 & 0 & 0 & 2p^2 \\ 0 & \frac{(1-p)^2}{8} & 0 & 0 & 0 & 0 & 0 & 0 \\ 0 & 0 & \frac{(1-p)^2}{8} & 0 & 0 & 0 & 0 & 0 \\ 0 & 0 & 0 & \frac{(1-p)^2}{8} & 0 & 0 & 0 & 0 \\ 0 & 0 & 0 & 0 & \frac{(1-p)^2}{8} & 0 & 0 & 0 \\ 0 & 0 & 0 & 0 & 0 & \frac{(1-p)^2}{8} & 0 & 0 \\ 0 & 0 & 0 & 0 & 0 & 0 & \frac{(1-p)^2}{8} & 0 \\ 2p^2 & 0 & 0 & 0 & 0 & 0 & 0 & \frac{(3p+1)^2}{8} \end{bmatrix}, \tag{S16}$$

which is also an "X"-shape density matrix. Thus, the GME concurrence of ρ'_{werner} can also be calculated as

$$C_{\text{GME}}(\rho'_{\text{werner}}) = \frac{1}{3p^2+1}\max\{0, 2p^2 - \frac{3}{8}(1-p)^2\}. \tag{S17}$$

To let $C_{\text{GME}}(\rho'_{\text{werner}}) > 0$, we can find that $p > \frac{4\sqrt{3}-3}{13} \sim 0.3022$. Therefore, in the range of $p \in (\frac{4\sqrt{3}-3}{13}, \frac{3}{7})$, the Werner state has the phenomenon of GME activation by collecting two copies. Note that $\frac{4\sqrt{3}-3}{13}$ may not be the lowest value of GME activation with two copies of ideal Werner states, as we derive it with a specific distillation protocol.

Now, we turn to analyze SLE. According to Eq. (S9), the calculation of SLE on subsystems A and B needs to search over all pure states on subsystem C, $|\psi_C\rangle = \cos\theta\,|0\rangle + \sin\theta e^{i\phi}\,|1\rangle$. For the ideal Werner state,

$$\frac{\langle\psi_C|\,\rho_{\text{werner}}\,|\psi_C\rangle}{\text{tr}(\langle\psi_C|\,\rho_{\text{werner}}\,|\psi_C\rangle)} = p(\cos\theta\,|00\rangle + \sin\theta e^{-i\phi}\,|11\rangle)(\cos\theta\,\langle 00| + \sin\theta e^{i\phi}\,\langle 11|) + \frac{1-p}{4}\mathbb{I}_2. \tag{S18}$$

It is easy to check that when searching over all the possible values of θ and ϕ, the maximal entanglement is obtained when $\theta = \frac{\pi}{4}$, with the state $\frac{p}{2}(|00\rangle + e^{-i\phi}\,|11\rangle)(\langle 00| + e^{i\phi}\,\langle 11|) + \frac{1-p}{4}\mathbb{I}_2$. It can be verified using the PPT criterion that when $p > \frac{1}{3}$, this two-qubit state is entangled. Therefore, the Werner state has SLE if and only if $p > \frac{1}{3}$.

According to Eq. (S16), after distillation, the ideal Werner state can be written as

$$\rho'_{\text{werner}} = \frac{3p^2+p}{3p^2+1}\left|G_0^+\right\rangle\!\left\langle G_0^+\right| + \frac{p-p^2}{3p^2+1}\left|G_0^-\right\rangle\!\left\langle G_0^-\right| + \frac{(1-p)^2}{8(3p^2+1)}\mathbb{I}_3. \tag{S19}$$

Thus, after the inner product with the reference state, we have

$$\frac{\langle\psi_C|\,\rho'_{\text{werner}}\,|\psi_C\rangle}{\text{tr}(\langle\psi_C|\,\rho'_{\text{werner}}\,|\psi_C\rangle)} = \frac{3p^2+p}{3p^2+1}\begin{bmatrix} \cos^2\theta & 0 & 0 & \frac{1}{2}\sin 2\theta e^{i\phi} \\ 0 & 0 & 0 & 0 \\ 0 & 0 & 0 & 0 \\ \frac{1}{2}\sin 2\theta e^{-i\phi} & 0 & 0 & \sin^2\theta \end{bmatrix} + \frac{p-p^2}{3p^2+1}\begin{bmatrix} \cos^2\theta & 0 & 0 & -\frac{1}{2}\sin 2\theta e^{i\phi} \\ 0 & 0 & 0 & 0 \\ 0 & 0 & 0 & 0 \\ -\frac{1}{2}\sin 2\theta e^{-i\phi} & 0 & 0 & \sin^2\theta \end{bmatrix} + \frac{(1-p)^2}{4(3p^2+1)}\mathbb{I}_2. \tag{S20}$$

To decide whether this state is entangled or not, we can take a partial transposition of this density matrix and calculate its lowest eigenvalue. The partial-transposed matrix is

$$\left[\frac{\langle\psi_C|\,\rho'_{\text{werner}}\,|\psi_C\rangle}{\text{tr}(\langle\psi_C|\,\rho'_{\text{werner}}\,|\psi_C\rangle)}\right]^{\text{T}_B} = \begin{bmatrix} \frac{2(p^2+p)}{3p^2+1}\cos^2\theta & 0 & 0 & 0 \\ 0 & 0 & \frac{2p^2}{3p^2+1}\sin 2\theta e^{-i\phi} & 0 \\ 0 & \frac{2p^2}{3p^2+1}\sin 2\theta e^{i\phi} & 0 & 0 \\ 0 & 0 & 0 & \frac{2(p^2+p)}{3p^2+1}\sin^2\theta \end{bmatrix} + \frac{(1-p)^2}{4(3p^2+1)}\mathbb{I}_2, \tag{S21}$$

whose lowest eigenvalue is

$$\lambda_{\min}\left\{\left[\frac{\langle\psi_C|\,\rho'_{\text{werner}}\,|\psi_C\rangle}{\text{tr}(\langle\psi_C|\,\rho'_{\text{werner}}\,|\psi_C\rangle)}\right]^{\text{T}_B}\right\} = \frac{(1-p)^2}{4(3p^2+1)} - \frac{2p^2}{3p^2+1}\sin 2\theta \geq \frac{(1-p)^2}{4(3p^2+1)} - \frac{2p^2}{3p^2+1}. \tag{S22}$$

If we require the lowest eigenvalue to be lower than 0, we have $p > \frac{2\sqrt{2}-1}{7} \sim 0.2612$. So in the region of $p \in (\frac{2\sqrt{2}-1}{7}, \frac{1}{3})$, two Werner states can be collected to activate SLE based on our distillation protocol. Similarly, $p = \frac{2\sqrt{2}-1}{7}$ may not be the lowest value for SLE activation with two copies, as we only consider a special distllation scheme here.

To clarify the conclusions, we use Fig. S1 to summarize ranges for different properties of the Werner state. In this diagram, we use $p^{(2)}_{\mathrm{GME}}$ and $p^{(2)}_{\mathrm{SLE}}$ to label the thresholds for using two copies of Werners states to active GME and SLE with our distillation protocol. Since it is only a special distillation protocol, these two values are upper bounds for entanglement activation thresholds with two copies. A meaningful problem is deriving the exact thresholds for SLE and GME activation with a finite number of copies. Besides, it has been proved that a multipartite state can always be used to activate GME given enough copies if and only if it is not separable in any fixed bi-partition, [7]. This means that $p^{(\infty)}_{\mathrm{GME}} = 0.2$ for the Werner state. Consequently, another important problem is that what is $p^{(\infty)}_{\mathrm{SLE}}$? In what condition can SLE not be activated even given an arbitrary number of the multipartite state? It is evident that a fully separable state has no SLE, so 0.2 is a lower bound for $p^{(\infty)}_{\mathrm{SLE}}$.

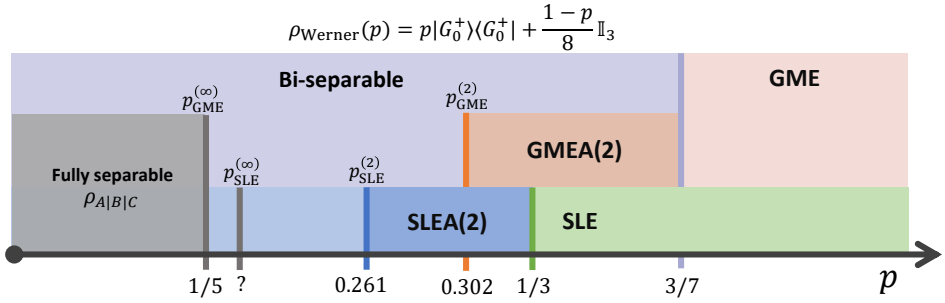

FIG. S1. Ranges of different properties for the Werner state.

V. ANALYSIS OF EXPERIMENTAL DISTILLATION FOR THE WERNER STATE

Previous theoretical and experimental works have demonstrated that bipartite entanglement distillation in polarization degrees of freedom of photons can be achieved with polarizing beam splitters (PBSs) [8–10]. Here, we present an analysis of the experimental tripartite distillation process for the three-photon Werner state prepared in polarization degrees of freedom.

The to-be-distilled Werner state can be decomposed into a mixture of eight GHZ states in Eq. (S10), where states $|0\rangle$ and $|1\rangle$ are encoded in $|H\rangle$ and $|V\rangle$ polarization of photons, respectively. Proportions of all these component states are $F_0^+ = \frac{1+7p}{8}$ and $F_0^- = F_1^+ = ... = F_3^- = \frac{1-p}{8} = F_r$, which are also fidelities between the Werner state and these component states. Among them, the state $\left|G_0^+\right\rangle$, with the largest fidelity of F_0^+, is the target state for the entanglement distillation.

As illustrated in Figure 2 in the main context, to perform the distillation operation, three clients superimpose their two photons on a PBS and post-select events where there is exactly one photon in each output of PBS. This requires the two photons to be in the same polarization, i.e., both $|0\rangle$ or both $|1\rangle$. As a result, the PBS operation, together with the post-selection, can be described using the projection operator $P = |00\rangle\langle 00| + |11\rangle\langle 11|$. The tripartite distillation allows two component states of two to-be-distilled Werner states to meet randomly on PBSs. From the polarization distribution of eight component states in Eq. (S10), we can see that the post-selection condition is satisfied only when the subscripts of two meeting component states are consistent, $\left|G_i^+\right\rangle$ and $\left|G_i^+\right\rangle$, $\left|G_i^+\right\rangle$ and $\left|G_i^-\right\rangle$, or $\left|G_i^-\right\rangle$ and $\left|G_i^-\right\rangle$. Other possible combinations of component states with different subscripts will be eliminated by post-selection, such as $\left|G_0^+\right\rangle$ meets $\left|G_1^+\right\rangle$. This can be verified mathematically by $P^{\otimes 3}\left|G_0^+\right\rangle\left|G_1^+\right\rangle = 0$.

After the post-selection, each client measures one of two output photons on the Pauli-X basis and compares the result. The Pauli-X measurement transforms the projection operator into either $P_+ = \langle +|\, P = \frac{1}{\sqrt{2}}(|0\rangle\langle 00| + |1\rangle\langle 11|)$ or $P_- = \langle -|\, P = \frac{1}{\sqrt{2}}(|0\rangle\langle 00| - |1\rangle\langle 11|)$. As stated in the main context, three clients keep the resultant three-photon state when an even number of $|-\rangle$ is recorded and apply a phase-flip operation when an odd number of $|-\rangle$ is recorded. Therefore, if $\left|G_i^+\right\rangle$ meets $\left|G_i^+\right\rangle$ or $\left|G_i^-\right\rangle$ meets $\left|G_i^-\right\rangle$ on PBSs, the resultant state will be $\left|G_i^+\right\rangle$; while if $\left|G_i^+\right\rangle$ meets $\left|G_i^-\right\rangle$, the resultant state will be $\left|G_i^-\right\rangle$. This can be verified with

$$\begin{aligned}
&(P_+P_+P_+ + P_+P_-P_- + P_-P_+P_- + P_-P_-P_+)\left|G_i^+\right\rangle \otimes \left|G_i^+\right\rangle \propto \left|G_i^+\right\rangle,\\
&(P_+P_+P_+ + P_+P_-P_- + P_-P_+P_- + P_-P_-P_+)\left|G_i^+\right\rangle \otimes \left|G_i^-\right\rangle \propto \left|G_i^-\right\rangle,\\
&(P_-P_-P_- + P_-P_+P_+ + P_+P_-P_+ + P_+P_+P_-)\left|G_i^+\right\rangle \otimes \left|G_i^+\right\rangle \propto \left|G_i^-\right\rangle,\\
&(P_-P_-P_- + P_-P_+P_+ + P_+P_-P_+ + P_+P_+P_-)\left|G_i^+\right\rangle \otimes \left|G_i^-\right\rangle \propto \left|G_i^+\right\rangle.
\end{aligned} \tag{S23}$$

Thus, after this whole distillation process, one obtains a new mixed state, which is a mixture of the same component states with new proportions $F_0^{+\prime}$, $F_0^{-\prime}$, $\cdots$, $F_3^{-\prime}$. For example, the fidelity for the target component state $\left|G_0^+\right\rangle$ becomes

$$F_0^{+\prime} = \frac{(F_0^+)^2 + (F_0^-)^2}{(F_0^+ + F_0^-)^2 + 3 \times (2F_r)^2} = \frac{(\frac{1+7p}{8})^2 + (\frac{1-p}{8})^2}{(\frac{1+7p}{8} + \frac{1-p}{8})^2 + 12 \times (\frac{1-p}{8})^2} = \frac{25p^2 + 6p + 1}{24p^2 + 8}, \tag{S24}$$

where the nominator is the probability of cases that $\left|G_0^+\right\rangle$ meets $\left|G_0^+\right\rangle$ and $\left|G_0^-\right\rangle$ meets $\left|G_0^-\right\rangle$, and the denominator represents the probability of the success of post-selection. One can prove that, for $p \in (\frac{4\sqrt{3}-3}{13}, \frac{3}{7}) \sim (0.3022, 0.4286)$, it holds that $F_0^+ < 0.5$ while $F_0^{+\prime} > 0.5$. This means the distilled state is genuinely entangled, while the to-be-distilled states are bi-separable. In other words, one can obtain genuine tripartite entanglement from two non-genuinely-entangled Werner states. This conclusion and the corresponding value interval are consistent with the theoretical analysis in Sec. IV.

VI. PREPARATION OF TO-BE-DISTILLED WERNER STATES

Here, we provide a detailed illustration of the Werner state preparation, using ρ_1 as an example. The procedure is depicted in Fig. S2. Initially, we generate a four-photon GHZ state $|\mathrm{GHZ}_4\rangle = \frac{1}{\sqrt{2}}(|HHHH\rangle + |VVVV\rangle)$ by interfering two photons from EPR_1 and EPR_2 on the PBS_1. With this state, we perform different measurements on the heralding photon t_1 to prepare different component states of the Werner state on a_1-b_1-c_1. Specifically, by introducing a HWP@22.5° in the light path of t_1, the following two scenarios arise:

(1) When $\mathrm{PBS}_{\mathrm{t}_1}$ is in the light path, the heralding photon t_1 will be triggered to state $|+\rangle$, and photons a_1-b_1-c_1 will be prepared as $\left|G_0^+\right\rangle = \frac{1}{\sqrt{2}}(|HHH\rangle + |VVV\rangle)$.

(2) When $\mathrm{PBS}_{\mathrm{t}_1}$ is removed from the light path, the heralding photon t_1 will be triggered to a mixed state $\rho_{\mathrm{t}_1} = \frac{1}{2}(|+\rangle\langle+| + |-\rangle\langle-|)$. In this case, photon t_1 directly enters the detector without polarization identification, resulting in the three-photon mixed state $\rho_{G_0} = \frac{1}{2}|H\rangle\langle H|^{\otimes 3} + \frac{1}{2}|V\rangle\langle V|^{\otimes 3} = \frac{1}{2}\left|G_0^+\right\rangle\left\langle G_0^+\right| + \frac{1}{2}\left|G_0^-\right\rangle\left\langle G_0^-\right|$ on photons a_1-b_1-c_1. With this state, we randomly insert two HWP@45° into light paths of photons a_1 and b_1 with the probability of 0.5, yielding three additional mixed states: $\rho_{G_1} = \frac{1}{2}\left|G_1^+\right\rangle\left\langle G_1^+\right| + \frac{1}{2}\left|G_1^-\right\rangle\left\langle G_1^-\right|$, $\rho_{G_2} = \frac{1}{2}\left|G_2^+\right\rangle\left\langle G_2^+\right| + \frac{1}{2}\left|G_2^-\right\rangle\left\langle G_2^-\right|$, and $\rho_{G_3} = \frac{1}{2}\left|G_3^+\right\rangle\left\langle G_3^+\right| + \frac{1}{2}\left|G_3^-\right\rangle\left\langle G_3^-\right|$. By randomly and equally preparing these four mixed states on photons a_1-b_1-c_1, we effectively prepare the three-photon maximally mixed state $\frac{\mathbb{I}_3}{8}$.

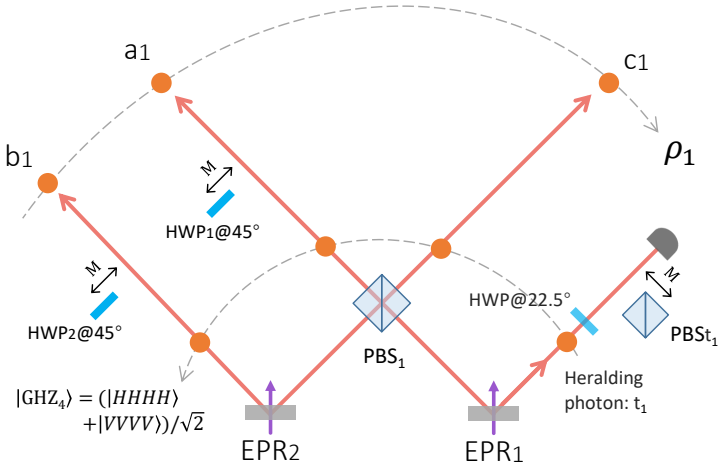

FIG. S2. Schematic diagram for the preparation of the to-be-distilled Werner state.

By combining the scenarios mentioned above (1) and (2) randomly with a specific probability, the desired Werner state $\rho_{\mathrm{werner}} = p\left|G_0^+\right\rangle\left\langle G_0^+\right| + (1-p)\frac{\mathbb{I}_3}{8}$ can be prepared. The detailed experimental settings are enumerated in Table S1. HWPs and PBSs are manipulated with a set of stepper motors. At the same time, random-number generators control the drivers of these motors to ensure the ideal mixture of the five components described above. Another to-be-distilled state can be obtained independently with EPR_3 and EPR_4 via the same method.

Output	Component states	Settings			Probability
		$\mathbf{PBS_{t1}}$	$\mathbf{HWP_1@45°}$	$\mathbf{HWP_2@45°}$	
$\left\|G_0^+\right\rangle$	$\frac{1}{\sqrt{2}}(\|HHH\rangle + \|VVV\rangle)$	in	out	out	$\frac{2p}{1+p}$
$\frac{\mathbb{I}_3}{8}$	$\rho_{G_0} = \frac{1}{2}\left\|G_0^+\right\rangle\!\left\langle G_0^+\right\| + \frac{1}{2}\left\|G_0^-\right\rangle\!\left\langle G_0^-\right\|$	out	out	out	$\frac{1-p}{4(1+p)}$
	$\rho_{G_1} = \frac{1}{2}\left\|G_1^+\right\rangle\!\left\langle G_1^+\right\| + \frac{1}{2}\left\|G_1^-\right\rangle\!\left\langle G_1^-\right\|$	out	in	out	$\frac{1-p}{4(1+p)}$
	$\rho_{G_2} = \frac{1}{2}\left\|G_2^+\right\rangle\!\left\langle G_2^+\right\| + \frac{1}{2}\left\|G_2^-\right\rangle\!\left\langle G_2^-\right\|$	out	out	in	$\frac{1-p}{4(1+p)}$
	$\rho_{G_3} = \frac{1}{2}\left\|G_3^+\right\rangle\!\left\langle G_3^+\right\| + \frac{1}{2}\left\|G_3^-\right\rangle\!\left\langle G_3^-\right\|$	out	in	in	$\frac{1-p}{4(1+p)}$

TABLE S1. Experimental settings for preparation of the Werner state ρ_1. p is the parameter of the target Werner state.

VII. TOMOGRAPHIC DATA

This section presents the reconstructed density matrices of to-be-distilled states with $p = 1$, $p = 0.5$, and $p = 0.36$. Fig. S3 can benchmark the state preparation process, like estimate parameters of q and r defined in Sec. III. Fig. S4 and Fig. S5 are employed to certify the GME and SLE activation phenomena, as discussed in Sec. III, respectively. For each to-be-distilled state, 27 measurement settings ($\sigma_x\sigma_x\sigma_x$, $\sigma_x\sigma_x\sigma_y$, $\sigma_x\sigma_x\sigma_z$, $\cdots$, $\sigma_z\sigma_z\sigma_z$) are applied. Data is collected for 5 minutes for each measurement setting for Fig. S3, and 3 hours for each measurement setting for Fig. S4 and Fig. S5.

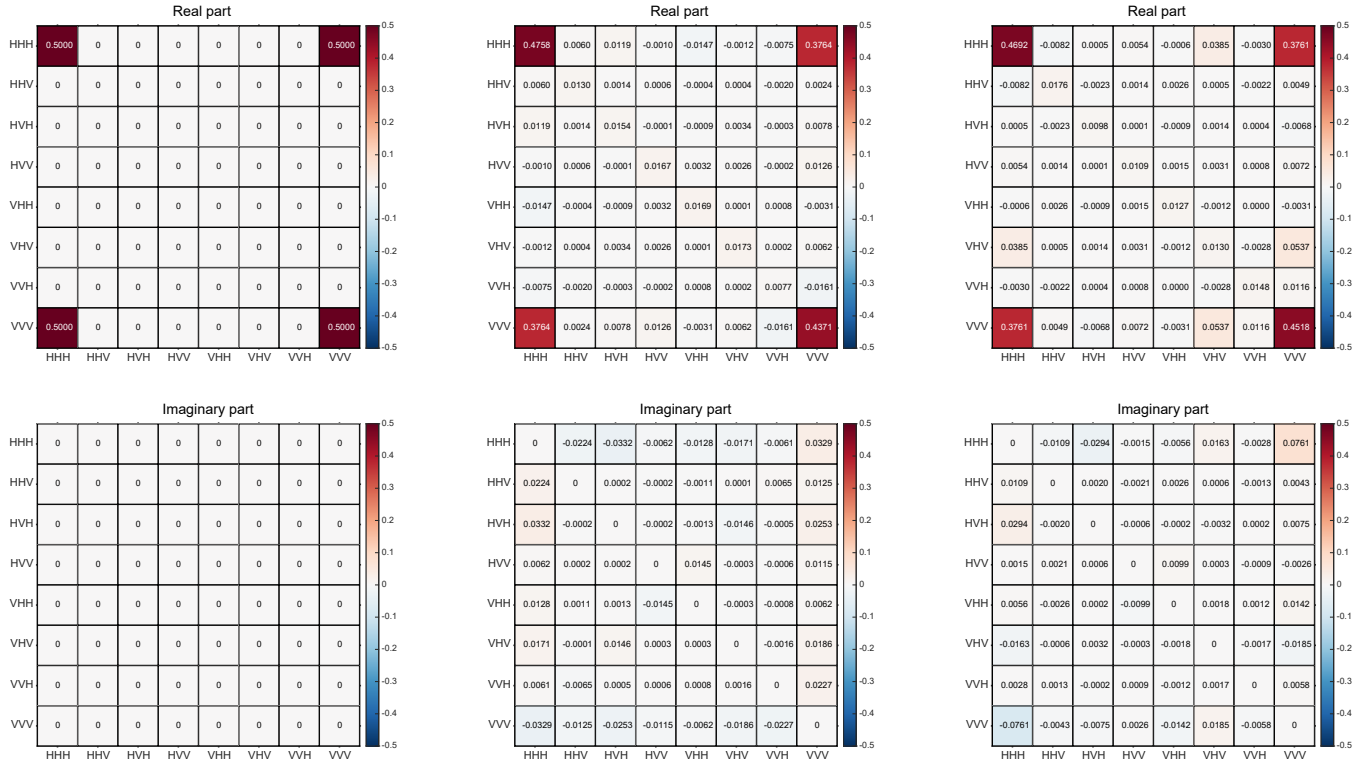

FIG. S3. **Left:** The density matrix of the Werner state with $p = 1$. **Middle:** Experimental reconstructed density matrix of ρ_1 with $p = 1$. **Right:** Experimental reconstructed density matrix of ρ_2 with $p = 1$.

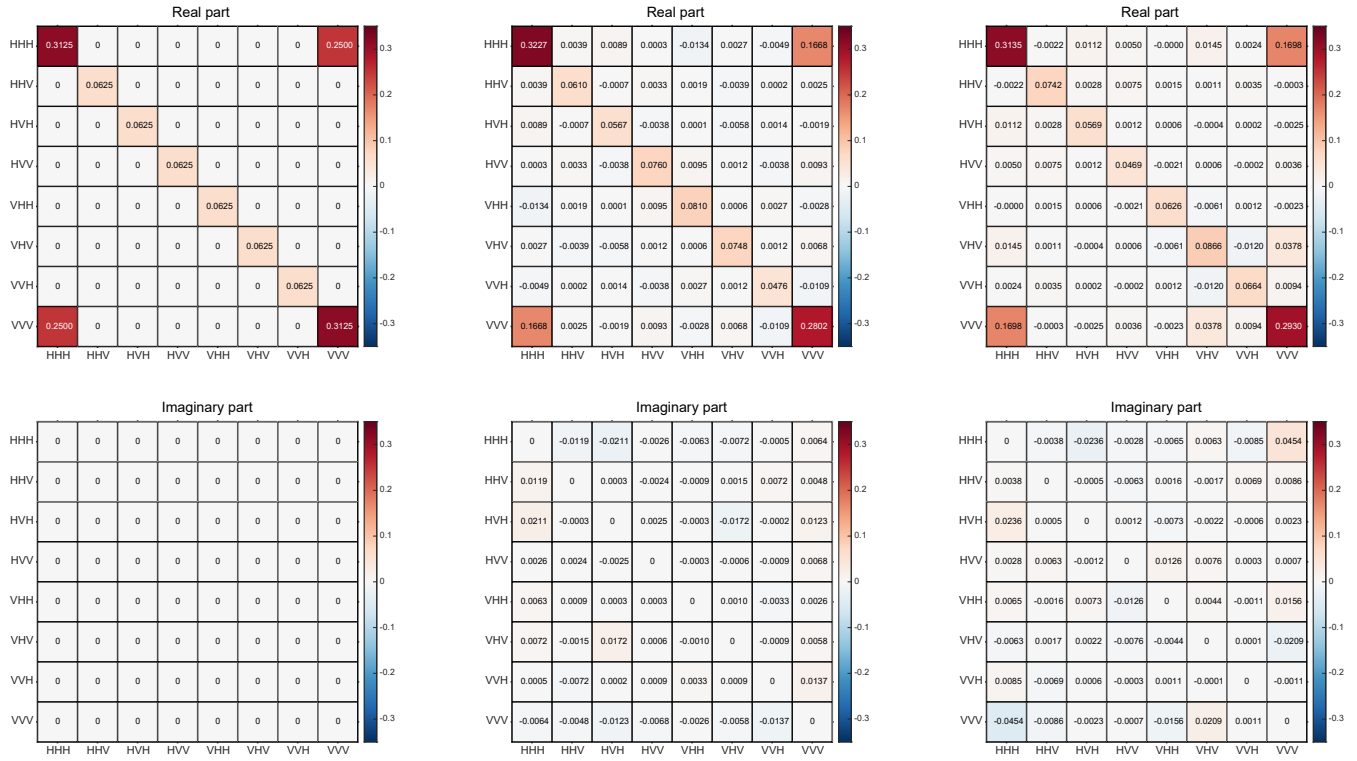

FIG. S4. **Left:** The density matrix of the Werner state with $p = 0.5$. **Middle:** Experimental reconstructed density matrix of ρ_1 with $p = 0.5$. **Right:** Experimental reconstructed density matrix of ρ_2 with $p = 0.5$.

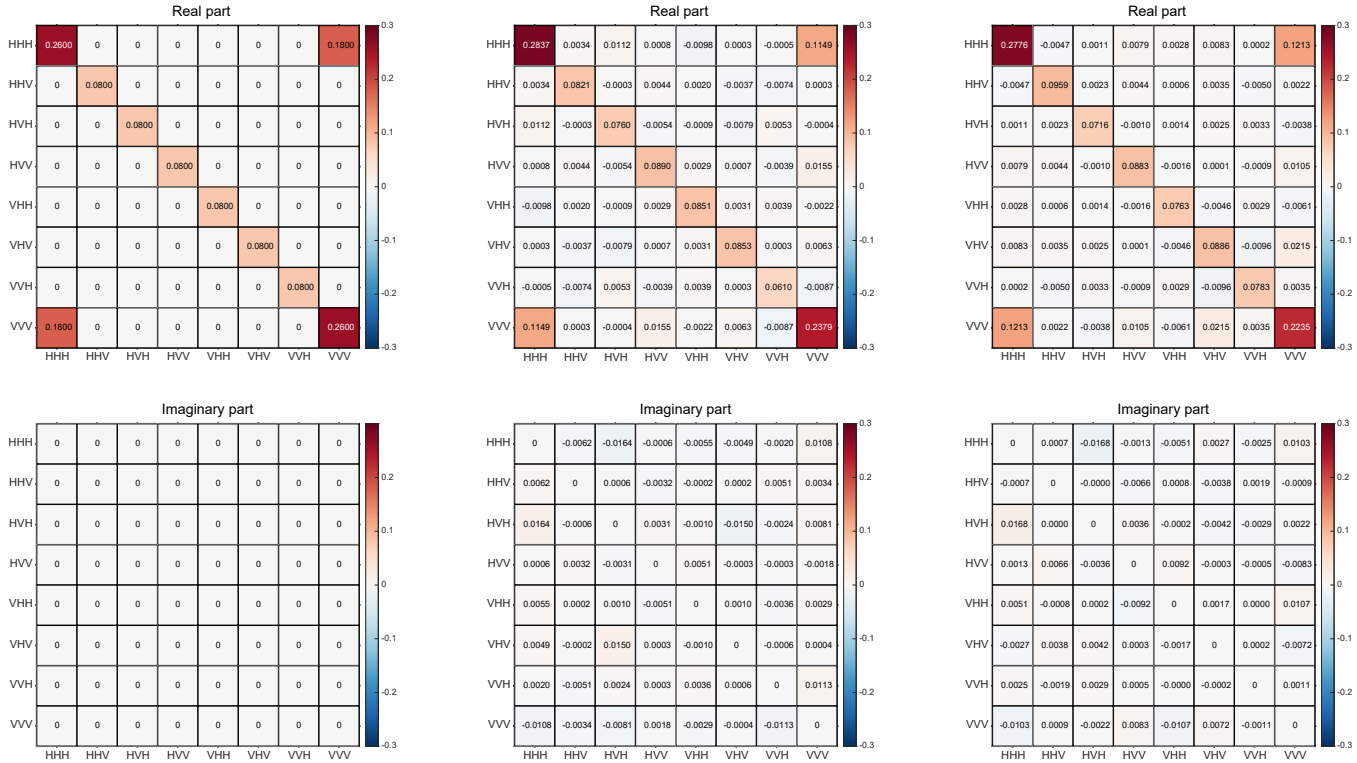

FIG. S5. **Left:** The density matrix of the Werner state with $p = 0.36$. **Middle:** Experimental reconstructed density matrix of ρ_1 with $p = 0.36$. **Right:** Experimental reconstructed density matrix of ρ_2 with $p = 0.36$.

[1] E. Chitambar, D. Leung, L. Mančinska, M. Ozols, and A. Winter, Communications in Mathematical Physics **328**, 303 (2014).
[2] H. Yamasaki, S. Morelli, M. Miethlinger, J. Bavaresco, N. Friis, and M. Huber, Quantum **6**, 695 (2022).
[3] Z.-H. Ma, Z.-H. Chen, J.-L. Chen, C. Spengler, A. Gabriel, and M. Huber, Phys. Rev. A **83**, 062325 (2011).
[4] S. M. Hashemi Rafsanjani, M. Huber, C. J. Broadbent, and J. H. Eberly, Phys. Rev. A **86**, 062303 (2012).
[5] B. Jungnitsch, T. Moroder, and O. Gühne, Phys. Rev. Lett. **106**, 190502 (2011).
[6] A. Peres, Phys. Rev. Lett. **77**, 1413 (1996).
[7] C. Palazuelos and J. I. d. Vicente, Quantum **6**, 735 (2022).
[8] J.-W. Pan, C. Simon, Č. Brukner, and A. Zeilinger, Nature **410**, 1067 (2001).
[9] J.-W. Pan, S. Gasparoni, R. Ursin, G. Weihs, and A. Zeilinger, Nature **423**, 417 (2003).
[10] L.-K. Chen, H.-L. Yong, P. Xu, X.-C. Yao, T. Xiang, Z.-D. Li, C. Liu, H. Lu, N.-L. Liu, L. Li, *et al.*, Nature Photonics **11**, 695 (2017).